Synthesis and Characterization of Mono-, Bis-, and Tetrakis-Pyridyltriarylporphyrin Pd(II) and Pt(II) Supramolecular Assemblies. Molecular Structure of a Pd-Linked Bisporphyrin Complex[1]

Hongping Yuan, Leonard Thomas, and L. Keith Woo*,[2]

Department of Chemistry, Iowa State University, Ames, Iowa 50011-3111

Received December 13, 1995[⊗]

A series of mono-, bis-, and tetrakisporphyrin assemblies was synthesized from 5-(*p*-pyridyl)-10,15,20-triphenylporphyrin, (pyPP)H_2, 5-(*p*-pyridyl)-10,15,20-tri(*p*-tolyl)porphyrin, (pyTP)H_2, (pyPP)Zn, (pyTP)Zn, and Pt(II) and Pd(II) complexes. Porphyrin subunits assemble around the central metal ions through the pyridyl group. Treating *trans*-Pd(DMSO)$_2$Cl$_2$ with 2 equiv of the pyridyl porphyrins resulted in the formation of *trans*-bisporphyrin assemblies Pd[(pyPP)H_2]$_2$Cl, Pd[(pyTP)H_2]$_2$Cl$_2$, Pd[(pyPP)Zn]$_2$Cl$_2$, and Pd[(pyTP)Zn]$_2$Cl$_2$. Treating *cis*-Pt(DMSO)$_2$Cl$_2$ with 1 equiv of each pyridylporphyrin produced the *cis*-monoporphyrin complexes Pt(DMSO)[(pyPP)H_2]Cl$_2$, Pt(DMSO)[(pyTP)H_2]Cl$_2$, Pt(DMSO)[(pyPP)Zn]Cl$_2$, and Pt(DMSO)[(pyTP)Zn]Cl$_2$. The treatment of Pt(DMSO)(pyPOR)Cl$_2$ with one more equiv of pyridylporphyrin resulted in the formation of *cis*-bisporphyrin assemblies, Pt[(pyPP)H_2]$_2$Cl$_2$, Pt[(pyTP)H_2]$_2$Cl$_2$, Pt[(pyPP)Zn]$_2$Cl$_2$, and Pt[(pyTP)Zn]$_2$Cl$_2$. Also, the reaction of Pt(DMSO)(pyPOR)Cl$_2$ and 4-pyridyl-4′-methylpyridinium iodide (MQ^+I^-) afforded *cis*-porphyrin−Pt−viologen assemblies. Treatment of M(DPPP)(OTf)$_2$ (M = Pt, Pd; DPPP = 1,3-bis(diphenylphosphino)propane; OTf = triflate anion) with 2 equiv of pyridylporphyrin resulted in *cis*-bisporphyrin assemblies [M(DPPP)[(pyPOR)H_2]$_2$](OTf)$_2$ and [M(DPPP)[(pyPOR)Zn]$_2$(OTf)$_2$. Synthesis of tetrakisporphyrin assemblies [M{(pyTP)H_2}$_4$]X_2 (M = Pt, Pd; X = BF_4, OTf) was accomplished by the reaction of [M(CH_3C$N)_4$]X_2 with (pyTP)H_2. Solution ^{1}H NMR studies show that the four porphyrins are equivalent and that the central metals have square planar geometry. The crystal structure of [Pd(DPPP){(pyTP)H_2}$_2$](OTf)$_2$ was determined by single-crystal X-ray diffraction analysis (monoclinic, $P2_1/n$, a = 13.211(5) Å, b = 36.741(19) Å, c = 22.971(10) Å, β = 91.54(3)°, V = 11145.8(86) Å^3, Z = 4, R = 8.21%, Rw = 18.44%).

Introduction

Understanding photoinduced electron transfer is a major scientific objective and is of technological importance for the design of synthetic molecular devices.[3] It is clear that the ability to mimic the natural photosynthesis process in the laboratory would have great technological significance in terms of solar energy conversion and storage. Synthetic porphyrin-based assemblies have been extensively used as models for molecular organization and energy/electron transfer processes.[4−8] Many clever and ingenious reaction center models have been prepared, and it is clear that the sophistication of synthetic multicomponent species that mimic the primary events of natural photosynthesis has increased tremendously. However, as the types and numbers of components are increased, the level of complexity also expands, and model systems become more difficult to prepare. To a large extent, progress in this area is still significantly synthesis limited. Most of the existing model systems are linked through organic spacers.[5−7] The synthetic methods for these systems typically are multistep processes, and yields are often extremely low. Recently some attempts have turned to developing new strategies for designing assemblies that can achieve sequential multistep electron transfer processes. Sessler *et al.* have prepared model systems that linked donors and acceptors through hydrogen bonds.[9] Sauvage *et al.* have designed bis(terpyridyl)porphyrins and utilized the terpyridyl group to build donor/acceptor arrays.[10]

Because separation and orientation are crucial factors in electron transfer,[11] we have developed new methods for utilizing transition metal coordination properties to place subunits at designated positions and at fixed distances. We report herein the synthesis of multiporphyrin and porphyrin−viologen assemblies linked in square planar arrays by Pd(II) or Pt(II) ions.

⊗ Abstract published in *Advance ACS Abstracts,* April 1, 1996.

(1) Part of this work was presented at the 207th American Chemical Society National Meeting, San Diego, CA, March 13−17, 1994, Yuan, H.; Woo, L. K. INOR 331.

(2) Presidential Young Investigator, 1990−1995: Camille and Henry Dreyfus Teacher−Scholar, 1993−1998.

(3) Fox, M. A.; Jones, W. E., Jr.; Watkins, D. M. *Chem. Eng. News* **1993**, *71* (11), 38.

(4) (a) Wagner, R. W.; Lindsey, J. S. *J. Am. Chem. Soc.* **1994**, *116*, 9759. (b) Seth, J.; Palaniappan, V.; Johnson, T. E.; Prathapan, S.; Lindsey, J. S.; Bocian, D. F. *J. Am. Chem. Soc.* **1994**, *116*, 10578. (c) Prathapan, S.; Johnson, T. E.; Lindsey, J. S. *J. AM. Chem. Soc.* **1993**, *115*, 7519. (d) Lindsey, J. S.; Prathapan, S.; Johnson, T. E.; Wagner, R. W. *Tetrahedron* **1994**, *50*, 8941.

(5) Wasielewski, M. R.; Gaines, G. L., III; Wiederrecht, G. P.; Svec, W. A.; Niemczyk, M. P. *J. Am. Chem. Soc.* **1993**, *115*, 10442.

(6) (a) Helms, A.; Heiler, D.; McLendon, G. *J. Am. Chem. Soc.* **1992**, *114*, 6227. (b) Helms, A.; Heiler, D.; McLendon, G. *J. Am. Chem. Soc.* **1991**, *113*, 4325. (c) McLendon, G. *Acc. Chem. Res.* **1988**, *21*, 160.

(7) (a) Sessler, J. L.; Johnson, M. R.; Creager, S. E.; Fettinger, J. C.; Ibers, J. A. *J. Am. Chem. Soc.* **1990**, *112*, 9310. (b) Sessler, J. L.; Capuano, V. L.; Harriman, A. *J. Am. Chem. Soc.* **1993**, *115*, 4618.

(8) (a) Osuka, A.; Maruyama, K. *J. Am. Chem. Soc.* **1988**, *110*, 4454. (b) Nagata, T.; Osuka, A.; Maruyama, K. *J. Am. Chem. Soc.* **1990**, *112*, 3054. (c) Osuka, A.; Maruyama, K.; Mataga, N.; Asahi, T.; Yamazaki, I.; Tamai, N. *J. Am. Chem. Soc.* **1990**, *112*, 4958. (d) Osuka, A.; Yamada, H.; Maruyama, K.; Mataga, N.; Asahi, T.; Ohkouchi, M.; Okada, T.; Yamazaki, I.; Nishimura, Y. *J. Am. Chem. Soc.* **1993**, *115*, 9439. (e) Osuka, A.; Nagata, T.; Maruyama, K. *Chem. Lett.* **1991**, 481. (f) Osuka, A.; Nagata, T.; Maruyama, K. *Chem. Lett.* **1991**, 1687. (g) Osuka, A.; Liu, B.-L.; Maruyama, K. *Chem. Lett.* **1993**, 949.

(9) (a) Sessler, J. L.; Wang, B.; Harriman, A. *J. Am. Chem. Soc.* **1993**, *115*, 10418. (b) Sessler, J. L.; Wang, B.; Harriman, A. *J. Am. Chem. Soc.* **1995**, *117*, 704.

(10) (a) Odobel, F.; Sauvage, J.-P.; Harriman, A. *Tetrahedron Lett.* **1993**, *34*, 8113. (b) Harriman, A.; Odobel, F.; Sauvage, J.-P. *J. Am. Chem. Soc.* **1994**, *116*, 5481. (c) Collin, J.-P.; Harriman, A.; Heitz, V.; Odobel, F.; Sauvage, J.-P. *J. Am. Chem. Soc.* **1994**, *116*, 5679.

S0020-1669(95)01594-1 CCC: $12.00 © 1996 American Chemical Society

The porphyrins used here are monopyridyltriarylporphyrins and the corresponding Zn complexes. A related series of compounds recently appeared.[12] In particular, the synthesis and partial characterization of $M[(pyPP)H_2]_2Cl_2$ and $M[(PyPP)Zn]_2Cl_2$ (M = Pd, Pt) were reported by Drain and Lehn in a preliminary communication. We include herein more complete characterization of these complexes, which were also reported by us earlier.[1]

Experimental Section

General. All reagents were analytical grade. THF and toluene were freshly distilled from purple solutions containing sodium and benzophenone. CH_3CN, CH_2Cl_2, and $CHCl_3$ were distilled from CaH_2. 5-(*p*-Pyridyl)-10,15,20-triphenylporphyrin (H_2pyPP) and 5-(*p*-pyridyl)-10,15,20-tritolylporphyrin (H_2pyTP) were synthesized according to a method reported elsewhere.[13] Column chromatography dimensions are reported in cm (length × diameter). The corresponding Zn metalloporphyrins were prepared by standard methods.[14] *cis*-$Pt(DMSO)_2Cl_2$,[15] *trans*-$Pd(DMSO)_2Cl_2$,[15] $Pt(DPPP)Cl_2$,[16] $Pd(DPPP)Cl_2$,[16] $Pt(DPPP)(OTf)_2$,[16] $Pd(DPPP)(OTf)_2$,[16] and $Pt(CH_3CN)_4(OTf)_2$[17] were prepared according to literature procedures.

UV−visible data were obtained using a Hewlett-Packard HP 8452A diode-array spectrophotometer. ^{1}H NMR spectra were recorded on a Nicolet NT300 spectrometer, a Varian VXR 300-MHz spectrometer, or a Bruker DRX 400-MHz spectrometer. Proton peak positions are referenced to TMS and assignments were made with the aid of 2D-COSY experiments. ^{31}P NMR spectra were recorded on a Bruker AC 200-MHz spectrometer, and all phosphorus chemical shifts are reported in ppm relative to external 85% H_3PO_4. IR spectra were recorded from KBR pellets on an IBM/Bruker IR-98 or a BIO-RAD Digilab FTS-7 spectrometer. Elemental analyses were performed by Atlantic Microlabs, Norcross, GA.

Preparations

5-(*p*-Pyridyl)-10,15,20-tritolylporphyrin (H_2pyTP). H_2pyTP was prepared according to a modified literature method[13] using *p*-tolualdehyde in place of benzaldehyde. Pyrrole (20.8 mL, 0.300 mol), *p*-tolualdehyde (23.6 mL, 0.200 mol), 4-pyridinecarboxaldehyde (6.6 mL, 0.080 mol), and 700 mL of propionic acid were added to a 2-L 3-necked round-bottom flask. The mixture was heated at reflux for 3 h, cooled to ambient temperature, and allowed to sit overnight. Purple crystals (7.0 g) were filtered and washed with cold methanol. Two-gram batches of this mixture were loaded on a flash chromatography column packed with silica gel (30 × 5 cm). CH_2Cl_2 was used to remove H_2TTP. Chloroform was used next to wash H_2pyTP off the column. The combined yield of H_2pyTP was 1.26 g (2.9%). ^{1}H NMR ($CDCl_3$, 300 MHz, ppm): 9.00 (d, 2H, J = 5.7 Hz, py-H_o), 8.89 (d, 2H, J = 4.8 Hz, β-H), 8.85 (s, 4H, β-H), 8.75 (d, 2H, J = 4.8 Hz, β-H), 8.14 (d, 2H, J = 5.7 Hz, py-H_m), 8.07 (d, 6H, J = 7.5 Hz, phenyl-H_o), 7.54 (d, 6H, J = 7.5 Hz, phenyl-H_m), 2.69 (s, 9H, Me), −2.82 (s, 2H, internal N*H*). UV−vis (CH_2Cl_2, nm): 418 (Soret), 482(s), 514, 548, 588, 646.

5-(*p*-Pyridyl)-10,15,20-triphenylporphyrinatozinc(II), Zn(pyPP). To a solution of H_2pyPP (250 mg, 0.400 mmol) in chloroform (100 mL) was added a saturated solution of zinc acetate (175 mg, 0.800 mmol) in methanol (5.0 mL). After 30 min of heating at reflux, the mixture was concentrated to about 3 mL, diluted with 10 mL of methanol, and cooled to −20 °C for 8 h. Purple crystals were filtered and washed with cold methanol to afford 265 mg of product (yield = 96%). ^{1}H NMR ($CDCl_3$, 300 MHz, ppm): 8.93 (s, 2H, β-H), 8.85 (m, 4H, β-H), 8.52 (d, 2H, J = 4.5 Hz, β-H), 8.20 (m, 2H, py-H_o), 8.08 (d, 6H, J = 6.6 Hz, phenyl-H_o), 7.77−7.62 (m, 11H, py-H_m, phenyl-$H_{m,p}$), 7.42 (bs, py-H_o from coordination oligomers), 6.24 (bs, py-H_m from coordination oligomers). (C_5D_5N, 300 MHz, ppm): 9.13 (d, 2H, J = 4.8 Hz, β-H), 9.10 (s, 6H, β-H, py-H_o), 9.03 (d, 2H, J = 4.8 Hz, β-H), 8.34 (m, 6H, phenyl-H_o), 8.24 (d, 2H, J = 5.7 Hz, py-H_m), 7.74 (m, 9H, phenyl-$H_{m,p}$). UV−vis (CH_2Cl_2, nm): 418 (Soret), 560, 604.

5-(*p*-Pyridyl)-10,15,20-tritolylporphyrinatozinc(II), Zn(pyTP). The same procedure for making Zn(pyPP) was employed using H_2pyTP (265 mg, 0.400 mmol) in place of H_2pyPP. Yield: 275 mg (95%). ^{1}H NMR ($CDCl_3$, 400 MHz, ppm): 8.86 (m, 6H, β-H), 8.55 (d, 2H, J = 4.4 Hz, β-H), 8.06 (d, 2H, J = 8.4 Hz, py-H_o), 7.97 (d, 6H, J = 7.2 Hz, phenyl-H_o), 7.50 (d, 6H, J = 7.2 Hz, phenyl-H_m), 7.45 (d, 2H, J = 8.4 Hz, py-H_m), 2.71 (s, 6H, 10,20-phenyl-Me), 2.63 (s, 3H, 15-phenyl-Me). (C_5D_5N, 400 MHz, ppm): 9.21 (s, 2H, β-H), 9.19 (s, 6H, β-H), 9.10 (d, 2H, J = 5.3 Hz, py-H_o), 9.04 (d, 2H, J = 5.3 Hz, py-H_m), 8.24 (d, 12 H, J = 6.9 Hz, phenyl-$H_{o,m}$), 2.54 (s, 9H, Me). UV−vis (CH_2Cl_2, nm): 422 (Soret), 562, 610.

***trans*-Pd[(pyPP)H$_2$]$_2$Cl$_2$.** *trans*-$Pd(DMSO)_2Cl_2$ (17 mg, 0.050 mmol) and H_2pyPP (62 mg, 0.10 mmol) were dissolved in 20 mL of $CHCl_3$ in a 50-mL round-bottom flask and heated at reflux for 4 h. The mixture was cooled to ambient temperature, and solvent was removed under reduced pressure. The residue was loaded on a silica column (25 × 2.5 cm) and eluted with $CHCl_3$. The first band was collected, and solvent was removed under reduced pressure. The product was recrystallized from CH_2Cl_2/hexane, filtered, washed with hexane, and air dried to give 70 mg (95% yield) of purple solid. R_f = 0.80 (on silica gel TLC, in $CHCl_3$). ^{1}H NMR ($CDCl_3$, 300 MHz, ppm): 9.39 (d, 4H, J = 6.3 Hz, py-H_o), 8.94 (d, 4H, J = 4.8 Hz, β-H), 8.86 (s, 8H, β-H), 8.83 (d, 4H, J = 4.8 Hz, β-H), 8.29 (d, 4H, J = 6.3 Hz, py-H_m), 8.21 (d, 12H, J = 7.2 Hz, phenyl-H_o), 7.78 (m, 18H, phenyl-$H_{m,p}$), 1.51 (s, 2H, H_2O), −2.81 (s, 4H, internal N*H*). UV−vis (CH_2Cl_2, nm): 420 (Soret), 484(s), 516, 552, 592, 646. IR (KBr): ν_{Pd-Cl} = 367 cm^{-1}. Anal. Calcd (found) for $C_{86}Cl_2H_{58}N_{10}Pd\cdot H_2O$: 72.40 (72.36); H, 4.24 (4.22); N, 9.82 (9.90).

***trans*-Pd[(pyPP)Zn]$_2$Cl$_2$.** *trans*-$Pd(DMSO)_2Cl_2$ (17 mg, 0.050 mmol) and Zn(pyPP) (68 mg, 0.10 mmol) were dissolved in 20 mL of $CHCl_3$ in a 50-mL round-bottom flask and heated at reflux for 2 h. The mixture was cooled to ambient temperature, and solvent was removed under reduced pressure. The residue is not soluble in most organic solvents except pyridine. The product was air dried to give 70 mg (91% yield) of purple solid. ^{1}H NMR (C_5D_5N, 300 MHz, ppm): 9.20−9.13 (m, 16H, β-H), 9.05 (d, 4H, J = 6.0 Hz, py-H_o), 8.37 (br, 12H, phenyl-H_o), 8.27 (d, 4H, J = 6.0 Hz, py-H_m), 7.76 (m, 18H, phenyl-$H_{m,p}$). UV−vis (pyridine, nm): 428 (Soret), 562, 602. MS {ESI} Calcd (found) *m*/*e*: 1619.7 (1620.6) $[MH]^+$.

***trans*-Pd[(pyTP)H$_2$]$_2$Cl$_2$.** A similar method for preparation of $Pd[(pyPP)H_2]_2Cl_2$ was used, replacing H_2pyPP with H_2pyTP (66 mg, 0.10 mmol). The product was isolated as a purple powder (69 mg, 92%). ^{1}H NMR ($CDCl_3$, 300 MHz, ppm): 9.38 (d, 4H, J = 6.3 Hz, py-H_o), 8.96 (d, 4H, J = 5.0 Hz, β-H),

(11) (a) Closs, G. L.; Miller, J. R. *Science* **1988**, *240*, 440. (b) Gust, D.; Moore, T. A. *Science* **1989**, *244*, 35. (c) Wasielewski, M. R. In *Photoinduced Electron Transfer*; Fox, M. A., Channon, M., Eds.; Elsevier: Amsterdam, 1988; Part A, Section 1.4. (d) Gust, D.; Moore, T. A. *Top. Curr. Chem.* **1991**, *159*, 103.
(12) Drain, C. M.; Lehn, J.-M. *J. Chem. Soc., Chem. Commun.* **1994**, 2313.
(13) Fleischer, E. B.; Schachter, A. M. *Inorg. Chem.* **1991**, *30*, 3763.
(14) Fuhrhop, J.; Smith, K. M. *Laboratory Methods in Porphyrin and Metalloporphyrin Research*; Elsevier: New York, 1975; p 42.
(15) Price, J. H.; Williamson, A. N.; Schramm, R. F.; Wayland, B. B. *Inorg. Chem.* **1972**, *11*, 1280.
(16) (a) Oliver, D. L.; Anderson, G. K. *Polyhedron* **1992**, *11*, 2415. (b) Fallis, S.; Anderson, G. K.; Rath, N. P. *Organometallics* **1991**, *10*, 3180.
(17) de Renzi, A. E.; Panunzi, A.; Vitagloano, A.; Paiaro, G. *J. Chem. Soc., Chem. Commun.* **1976**, 47.

8.88 (s, 8H, β-H), 8.81 (d, 4H, $J = 5.0$ Hz, β-H), 8.28 (d, 4H, $J = 6.4$ Hz, py-H_m), 8.10 (d, 8H, $J = 7.8$ Hz, 10,20-phenyl-H_o), 8.08 (d, 4H, $J = 7.8$ Hz, 15-phenyl-H_o), 7.58 (d, 8H, $J = 7.8$ Hz, 10,20-phenyl-H_m), 7.55 (d, 4H, $J = 7.8$ Hz, 15-phenyl-H_m), 2.72 (s, 12H, 10,20-phenyl-Me) 2.70 (s, 6H, 15-phenyl-Me), −2.79 (s, 4H, internal N*H*). UV−vis (CH_2Cl_2, nm): 422 (Soret), 484(s), 518, 554, 592, 648. MS {ESI} Calcd (found) *m*/*e*: 1490.4 (1491.0) $[MH]^+$.

***cis*-Pt(DMSO)[(pyPP)H$_2$]Cl$_2$.** *cis*-Pt(DMSO)$_2$Cl$_2$ (42 mg, 0.10 mmol) and H_2pyPP (62 mg, 0.10 mmol) were dissolved in 20 mL of CH_2Cl_2 in a 50-mL round-bottom flask and stirred for 4 h at ambient temperature. The solvent was removed under reduced pressure, and the solid residue was loaded on a silica column (25 × 2.5 cm) and eluted with $CHCl_3$/ethyl acetate (5:1). The second band was collected and taken to dryness under reduced pressure. The product was recrystallized from CH_2Cl_2/hexane to afford 92 mg (95% yield) of purple solid. $R_f = 0.35$ (silica gel TLC, in $CHCl_3$). ^{1}H NMR ($CDCl_3$, 300 MHz, ppm): 9.17 (d, 2H, $J = 6.5$ Hz, py-H_o), 8.91 (d, 2H, $J = 4.8$ Hz, β-H), 8.84 (s, 4H, β-H), 8.74 (d, 2H, $J = 4.8$ Hz, β-H), 8.28 (d, 2H, $J = 6.5$ Hz, py-H_m), 8.19 (d, 6H, $J = 7.2$ Hz, phenyl-H_o), 7.77 (m, 9H, phenyl-$H_{m,p}$), 3.60 (s, 6H, DMSO), −2.83 (s, 2H, internal N_H). UV−vis (CH_2Cl_2, nm): 420 (Soret), 484(s), 516, 552, 590, 646.

***cis*-Pt(DMSO)[(pyTP)H$_2$]Cl$_2$.** H_2pyTP (66 mg, 0.10 mmol) was used in place of H_2pyPP, in a similar method for the preparation of *cis*-Pt(DMSO)(H_2pyPP)Cl_2. Yield: 90 mg (90%). ^{1}H NMR ($CDCl_3$, 300 MHz, ppm): 9.15 (d, 2H, $J = 5.9$ Hz, py-H_o), 8.92 (d, 2H, $J = 4.5$ Hz, β-H), 8.86 (s, 4H, β-H), 8.72 (d, 2H, $J = 4.5$ Hz, β-H), 8.26 (d, 2H, $J = 5.9$ Hz, py-H_m), 8.06 (d, 6H, $J = 7.5$ Hz, phenyl-H_o), 7.55 (d, 6H, $J = 7.5$ Hz, phenyl-H_m), 3.60 (s, 6H, DMSO), 2.69 (s, 9H, Me), 1.50 (s, 2H, H_2O), −2.82 (s, 2H, internal N*H*). UV−vis (CH_2Cl_2, nm): 422 (Soret), 484(s), 518, 554, 592, 648. Anal. Calcd (found) for $C_{48}Cl_2H_{41}N_5OSPt\cdot H_2O$: C, 56.53 (56.25); H, 4.25 (4.20); N, 6.87 (6.86). MS {ESI} Calcd. (found) *m*/*e*: 1000.9 (1001.9) $[MH]^+$.

***cis*-Pt(DMSO)[(pyPP)Zn]Cl$_2$.** A similar procedure for the preparation of Pt(DMSO)[(pyPP)H_2]Cl_2 was employed, using Zn(pyPP) (68 mg, 0.10 mmol) in place of H_2pyPP. Yield: 96 mg (93%). ^{1}H NMR ($CDCl_3$, 300 MHz, ppm): 9.14 (d, 2H, $J = 6.8$ Hz, py-H_o), 9.01 (d, 2H, $J = 4.8$ Hz, β-H), 8.94 (m, 4H, β-H), 8.84 (d, 2H, $J = 4.8$ Hz, β-H), 8.28 (d, 2H, $J = 6.8$ Hz, py-H_m), 8.19 (m, 6H, phenyl-H_o), 7.75 (m, 9H, phenyl-$H_{m,p}$), 3.56 (s, 6H, DMSO). UV−vis (CH_2Cl_2, nm): 420 (Soret), 548, 588.

***cis*-Pt(DMSO)[(pyTP)Zn]Cl$_2$.** A similar procedure for the preparation of Pt(DMSO)[(pyPP)H_2]Cl_2 was employed, using Zn(pyTP) (72 mg, 0.10 mmol) in place of H_2pyPP. Yield: 98 mg (92%). ^{1}H NMR ($CDCl_3$, 400 MHz, ppm): 9.14 (d, 2H, $J = 5.8$ Hz, py-H_o), 9.02 (d, 2H, $J = 4.4$, β-H), 8.96 (s, 4H, β-H), 8.82 (d, 2H, $J = 4.4$ Hz, β-H), 8.27 (d, 2H, $J = 5.8$ Hz, py-H_m), 8.07 (d, 6H, $J = 7.4$ Hz, phenyl-H_o), 7.55 (d, 6H, $J = 7.4$ Hz, phenyl-H_m), 3.58 (s, 6H, DMSO), 2.70 (s, 9H, Me), 1.50 (s, 2H, H_2O). UV−vis (CH_2Cl_2, nm): 420 (Soret), 548, 588. Anal. Calcd (found) for $C_{48}Cl_2H_{39}N_5OSPtZn\cdot H_2O$: C, 53.22 (52.98); H, 3.81 (3.77); N, 6.40 (6.47). MS {ESI} Calcd (found) *m*/*e*: 1065.3 (1066) $[MH]^+$.

***cis*-Pt[(pyPP)H$_2$]$_2$Cl$_2$.** Method A. *cis*-Pt(DMSO)$_2$Cl$_2$ (21 mg, 0.050 mmol) and H_2pyPP (62 mg, 0.10 mmol) were dissolved in 20 mL of toluene in a 50-mL round-bottom flask and heated at reflux for 36 h. The mixture was cooled to ambient temperature, and solvent was removed under reduced pressure. The residue was loaded on a silica column (25 × 2.5 cm) and eluted with $CHCl_3$. The first band was collected and taken to dryness under reduced pressure. The product was recrystallized from CH_2Cl_2/hexane to afford 72 mg (96% yield) of purple solid. Method B. Pt(DMSO)(H_2pyPP)Cl_2 (50 mg, 0.050 mmol) was added to the solution of H_2pyPP (32 mg, 0.050 mmol) in toluene (20 mL) and heated at reflux for 36 h. The product was isolated as described in method A to afford 65 mg (87% yield) of purple solid. $R_f = 0.84$ (silica gel TLC, in $CHCl_3$). ^{1}H NMR ($CDCl_3$, 300 MHz, ppm): 9.47 (d, 4H, $J = 6.2$ Hz, py-H_o), 8.96 (d, 4H, $J = 4.8$ Hz, β-H), 8.86 (m, 12H, β-H), 8.26 (d, 4H, $J = 6.2$ Hz, py-H_m), 8.22 (m, 12H, phenyl-H_o), 7.78 (m, 18H, phenyl-$H_{m,p}$), −2.80 (s, 4H, internal N*H*). UV−vis (CH_2Cl_2, nm): 420 (Soret), 484(s), 516, 552, 590, 646. IR (KBr): $\nu_{Pt-Cl} = 354$, 324 cm^{-1}. MS {ESI} Calcd (found) *m*/*e*: 1495.4 (1496) $[MH]^+$.

***cis*-Pt[(pyTP)H$_2$]$_2$Cl$_2$.** Method A for the preparation of *cis*-Pt[(pyPP)H_2]$_2Cl_2$ was used, except H_2pyTP (66 mg,0.10 mmol) was substituted for H_2pyPP. Yield: 74 mg of purple product (93%). ^{1}H NMR ($CDCl_3$, 300 MHz, ppm): 9.46 (d, 4H, $J = 6.3$ Hz, py-H_o), 8.96 (d, 4H, $J = 4.8$ Hz, β-H), 8.87 (s, 8H, β-H), 8.83 (d, 4H, $J = 4.8$ Hz, β-H), 8.25 (d, 4H, $J = 6.3$ Hz, py-H_m), 8.08 (d, 12H, $J = 7.8$ Hz, phenyl-H_o), 7.57 (m, 12H, phenyl-H_m), 2.72 (s, 12H, 10,20-phenyl-Me), 2.70 (s, 6H, 15-phenyl-Me), −2.79 (s, 4H, internal N*H*). UV−vis (CH_2Cl_2, nm): 422 (Soret), 484(s), 518, 554, 592, 649. Anal. Calcd (found) for $C_{92}Cl_2H_{70}N_{10}Pt$: C, 69.87 (69.38); H, 4.48 (4.38); N, 8.86 (8.58). MS {ESI} Calcd (found) *m*/*e*: 1579 (1579) $[M]^+$.

***cis*-Pt[(pyPP)H$_2$](MQ$^+$I$^-$)Cl$_2$.** *cis*-Pt(DMSO)(H_2pyPP)Cl_2 (37 mg, 0.037 mmol) was added to a boiling solution of 4-pyridyl-4′-methylpyridinium iodide (MQ^+I^-) (45 mg, 0.15 mmol) in 25 mL of THF/EtOH (1:1 v/v). The mixture was heated at reflux under N_2 for 12 h. After removing the solvent under reduced pressure, the residue was dissolved in CH_2Cl_2 and filtered to remove excess 4-pyridyl-4′-methylpyridinium iodide. This process was repeated twice to produce a purple solid (30 mg, 70%). ^{1}H NMR ($CDCl_3$, 300 MHz, ppm): 9.51 (d, 2H, $J = 5.4$ Hz, py-H_o), 8.97 (d, 2H, $J = 5.6$ Hz, MQ-H_o), 8.86 (m, 2H, MQ-$H_{o'}$), 8.84 (m, 6H, β-H), 8.77 (d, 2H, $J = 5.1$ Hz, β-H), 8.19 (m, 8H, py-H_m, phenyl-H_o), 8.14 (d, 2H, $J = 5.6$ Hz, MQ-H_m), 7.76 (m, 9H, phenyl-$H_{m,p}$), 7.61 (d, 2H, $J = 6.0$ Hz, MQ-$H_{m'}$), 4.78 (s, 3H, MQ-Me), −2.84 (s, 2H, internal N*H*). UV−vis (CH_2Cl_2 nm): 418 (Soret), 514, 548, 588, 644.

***cis*-Pt[(pyTP)H$_2$](MQ$^+$I$^-$)Cl$_2$.** A similar method for the preparation of Pt[(pyPP)H_2](MQ^+I^-)Cl_2 was employed, using Pt(DMSO)H_2pyTP) (37 mg, 0.037 mmol) in place of Pt(DMSO)(H_2pyPP)Cl_2. Yield: 23 mg (51%). ^{1}H NMR ($CDCl_3$, 300 MHz, ppm): 9.42 (d, 2H, $J = 6.3$, py-H_o), 8.97 (d, 2H, $J = 5.4$ Hz, MQ-H_o), 8.89 (d, 2H, $J = 5.6$ Hz, MQ-$H_{o'}$), 8.85 (m, 6H, β-H), 8.75 (d, 2H, J = 4.5 Hz, β-H), 8.19 (d, 2H, $J = 5.4$ Hz, MQ-H_m), 8.14 (d, 2H, $J = 6.3$ Hz, py-H_m), 8.07 (d, 6H, $J = 7.8$ Hz, phenyl-H_o), 7.59 (d, 2H, $J = 5.6$ Hz, MQ-$H_{m'}$), 7.53 (d, 6H, $J = 7.8$ Hz, phenyl-H_m), 4.73 (s, 3H, MQ-Me), 2.69 (s, 9H, Me), −2.83 (s, 2H, internal N*H*). UV−vis (CH_2Cl_2, nm): 418 (Soret), 514, 548, 588, 644.

***cis*-Pt[(pyPP)Zn](MQ$^+$I$^-$)Cl$_2$.** This complex was prepared from Pt(DMSO)[(pyPP)Zn]Cl_2 (29 mg, 0.028 mmol) and 4-pyridyl-4′-methylpyridinium iodide (34 mg, 0.12 mmol) by the same method used for the preparation of Pt[(pyPP)H_2](MQ^+I^-)Cl_2. Yield: 25 mg (72%). ^{1}H NMR ($CDCl_3$, 400 MHz, ppm): 9.37 (br, 2H, py-H_o), 8.85 (m, 6H, β-H), 8.54 (br, 2H, β-H), 8.37 (br, 2H, MQ-H_o), 8.18 (d, 2H, $J = 6.8$ Hz, MQ-$H_{o'}$), 8.09 (d, 8H, $J = 6.4$ Hz, py-H_m, phenyl-H_o), 7.74−7.65 (m, 11H, MQ-$H_{m'}$, phenyl-$H_{m,p}$), 7.43 (d, 2H, $J = 4.8$ Hz, MQ-H_m), 4.67 (s, 3H, MQ-Me). Peak assignments for MQ-H_o and MQ-H_m are less certain because cross peaks were too weak to

be observed in the 2D-COSY experiment. UV−vis (CH_2Cl_2, nm): 418 (Soret), 550, 606.

***cis*-Pt[(pyTP)Zn](MQ$^+$I$^-$)Cl$_2$.** A similar method for the preparation of Pt[(pyPP)Zn](MQ$^+$I$^-$)Cl_2 was employed, using Pt(DMSO)[Zn(pyTP)]Cl_2 (30 mg, 0.028 mmol) in place of Pt(DMSO)[Zn(pyPP)]Cl_2. Yield: 22 mg (60%). ^{1}H NMR ($CDCl_3$, 400 MHz, ppm): 9.10 (d, 2H, J = 6.2 Hz, py-H$_o$), 8.88 (m, 8H,MQ-H$_o$, β-H), 8.67 (d, 2H, J = 4.8 Hz, β-H), 8.60 (br, 2H, MQ-H$_{o'}$), 8.07 (d, 2H, J = 6.2 Hz, py-H$_m$), 8.04 (d, 6H, J = 7.6 Hz, phenyl-H$_o$), 7.98 (m, 2H, MQ-H$_m$), 7.50 (m, 8H, phenyl-H$_m$, MQ-H$_{m'}$), 4.55 (s, 3H, MQ-Me), 2.68 (s, 9H, phenyl-Me). Assignments for MQ-H$_{o'}$ and MQ-H$_{m'}$ are less certain because cross peaks in the 2D-COSY spectrum were too weak to be observed. UV-vis (CH_2Cl_2, nm): 418 (Soret), 552, 606. Anal. Calcd (found) for $C_{57}Cl_2H_{44}IN_7PtZn$: C, 53.47 (53.92); H, 3.65 (3.99); N, 7.98 (8.44).

[*cis*-Pd(DPPP)[(pyTP)H$_2$]$_2$](OTf)$_2$ Pd(DPPP)Cl_2 (60 mg, 0.10 mmol) and Ag(OSO_2CF_3) (53 mg, 0.21 mmol) were dissolved in 50 mL of CH_2Cl_2, and the mixture was stirred under argon in the dark for 3 h. AgCl was removed by filtration, and the filtrate was concentrated to 5 mL. H_2pyTP (135 mg, 0.210 mmol) and 50 mL of acetone were added to the filtrate, and the mixture was stirred at room temperature for 5 h. Solvent was removed under reduced pressure, and the residue was recrystallized from CH_2Cl_2/hexane. The production was a purple solid (196 mg, 92%). ^{1}H NMR ($CDCl_3$, 300 MHz, ppm): 9.61 (d, 4H, J = 6.6 Hz, py-H$_o$), 8.83 (d, 8H, J = 4.8 Hz, β-H), 8.75 (br, 4H, β-H), 8.22 (br, 4H, β-H), 8.08 (m, 24H, py-H$_m$, porphyrin phenyl-H$_o$, DPPP-phenyl-H$_o$), 7.63 (t, 12H, J = 7.4 Hz, DPPP-phenyl-H$_{m,p}$), 7.55 (d, 12H, J = 7.8 Hz, porphyrin phenyl-H$_m$), 3.47 (m, 4H, CH_2-P), 2.70 (s, 18H, Me), 2.49 (m, 2H, CH_2), −2.88 (s, 4H, internal N*H*). ^{31}P NMR (acetone-d_6, ppm): 6.91. UV−vis (CH_2Cl_2, nm): 420 (Soret), 518, 554, 592, 648.

[*cis*-Pd(DPPP)[(pyTP)Zn]$_2$](OTf)$_2$. [*cis*-Pd(DPPP)[(pyTP)-Zn]$_2$](OTf)$_2$ was prepared analogously to [Pd(DPPP)(H$_2$pyTP)$_2$]-(OTf)$_2$, except that Zn(pyTP) (150 mg, 0.210 mmol) was added to the Pd(DPPP)(OTf)$_2$ solution. Yield: 203 mg of purple powder (90%). ^{1}H NMR ($CDCl_3$, 400 MHz, ppm): 9.57 (d, 4H, J = 6.0 Hz, py-H$_o$), 8.96 (s, 8H, β-H), 8.84 (m, 4H, β-H), 8.54 (br, 4H, β-H), 8.11−7.90 (m, 24H, porphyrin phenyl-H$_o$, DPPP-phenyl-H$_o$, py-H$_m$), 7.66−7.35 (m, 24H, porphyrin phenyl-H$_m$, DPPP-phenyl-H$_{m,p}$), 3.45 (m, 4H, CH_2−P), 2.70 (s, 12H, 10,20-phenyl-Me), 2.66 (br, 2H, CH_2), 2.63 (s, 6H, 15-phenyl-Me). ^{31}P NMR ($CDCl_3$, ppm): 5.28. UV−vis (CH_2Cl_2, nm): 422 (Soret), 550, 592. MS {ESI} Calcd (found) *m*/*e*: 2261.1 (2262) [MH]$^+$.

[*cis*-Pt(DPPP)(H$_2$pyTP)$_2$](OTf)$_2$. [*cis*-Pt(DPPP)(H$_2$pyTP)$_2$]-(OTf)$_2$ was prepared analogously to [Pd(DPPP)(H$_2$pyTP)$_2$]-(OTf)$_2$. However, Pt(DPPP)Cl_2 (68 mg, 0.10 mmol) was used. Yield: 195 mg of purple powder (86%). ^{1}H NMR ($CDCl_3$, 400 MHz, ppm): 9.68 (d, 4H, J = 4.6 Hz, py-H$_o$), 8.86 (m, 8H, β-H), 8.75 (br, 4H, β-H), 8.24 (br, 4H, β-H), 8.15 (d, 4H, J = 4.6 Hz, py-H$_m$), 8.07 (d, 20H, PPh$_2$-H$_o$, porphyrin phenyl-H$_o$), 7.64 (t, 12H, J = 7.2 Hz, PPh$_2$-H$_{m,p}$), 7.54 (m, 12 H, porphyrin phenyl H$_m$), 3.54 (m, 4H, CH_2−P), 2.70 (s, 18H, Me), 2.47 (m, 2H, CH_2), −2.87 (s, 4H, interal N*H*). ^{31}P NMR (acetone-d_6, ppm): −15.00 (J_{Pt-P} = 3235 Hz). UV−vis (CH_2Cl_2, nm): 420 (Soret), 448, 518, 550, 592, 650. MS {ESI} Calcd (found) *m*/*e*: 960.8 (961) [(M-2OTf)]$^{2+}$.

[*cis*-Pt(DPPP)[Zn(pyTP)]$_2$](OTf)$_2$. [*cis*-Pt(DPPP)[Zn(pyTP)]$_2$]-(OTf)$_2$ was synthesized analogously to [Pt(DPPP)(H$_2$pyTP)$_2$]-(OTf)$_2$, except that Zn(pyTP) (150 mg, 0.210 mmol) was added to the Pt(DPPP)(OTf)$_2$ solution. Yield: 213 mg of purple powder (90%). ^{1}H NMR ($CDCl_3$, 400 MHz, ppm): 9.63 (d, 4H, J = 6.0 Hz, py-H$_o$), 8.94 (br, 8H, β-H), 8.80 (m, 4H, β-H), 8.54 (m, 4H, β-H), 8.15 (d, 4H, J = 6.0 Hz, py-H$_m$), 8.09 (d, 20H, J = 7.8 Hz, PPh$_2$-H$_o$, porphyrin phenyl-H$_o$), 7.66 (m, 12H, PPh$_2$-H$_{m,p}$), 7.49 (m, 12H, porphyrin H$_m$), 3.55 (m, 4H, CH_2−P), 2.70 (s, 18H, Me), 2.63 (m, 2H, CH_2). ^{31}P NMR ($CDCl_3$, ppm): −16.47. UV−vis (CH_2Cl_2, nm): 422 (Soret), 552, 594.

{Pd[(pyTP)H$_2$]$_4$}(BF$_4$)$_2$. [Pd(CH_3CN)$_4$](BF$_4$)$_2$ (20 mg, 0.045 mmol) and H_2pyTP (120 mg, 0.180 mmol) were heated at reflux in toluene (30 mL) for 2 days under Ar. Solvent was removed under reduced pressure, and the residue was dissolved in a minimum amount (∼3 mL) of C_6H_6. Diethyl ether and hexane (1:1, 10 mL) were added, and the mixture was cooled to −20 °C for 8 h. Filtering and washing the solid with diethyl ether produced a purple powder (112 mg, 85%). ^{1}H NMR (CD_2Cl_2, 400 MHz, ppm): 10.35 (d, 2H, J = 6.0 Hz, py-H$_o$), 8.89 (m, 6H, β-H), 8.81 (d, 2H, J = 6.0 Hz, py-H$_m$), 8.75 (d, J = 4.4, β-H), 8.11 (m, 4H, 10,20-phenyl-H$_o$), 7.87 (d, 2H, J = 7.5 Hz, 15-phenyl-H$_o$), 7.61 (m, 4H, 10,20-phenyl-H$_m$), 7.25 (d, 2H, J = 7.8 Hz, 15-phenyl-H$_m$), 2.71 (s, 6H 10,20-phenyl-Me), 2.43 (s, 3H, 15-phenyl-Me), −2.78 (s, 2H, internal N*H*). UV−vis (CH_2Cl_2, nm): 420 (Soret), 484 (shoulder), 518, 556, 592, 650.

[Pt(H$_2$pyTP)$_4$](OTf)$_2$ [Pt(CH_3CN)$_4$](OTf)$_2$ (20 mg, 0.030 mmol) and H_2pyTP (82 mg, 0.12 mmol) were heated at reflux in toluene/CH_2Cl_2 (v/v: 1:1, 40 mL) for 12 h under Ar. The solvent was removed under reduced pressure, and the residue was dissolved in a minimum amount (2−5 mL) of CH_2Cl_2. Diethyl ether and hexane were added (10−15 mL), and the mixture was cooled to −20 °C for 8 h. Filtering and washing the solid with diethyl ether produced a purple powder (75 mg, 80%). ^{1}H NMR (CD_2Cl_2, 300 MHz, ppm): 10.52 (d, 2H, J = 6.0 Hz, py-H$_o$), 8.91 (m, 4H, β-H), 8.84 (d, 2H, J = 4.8 Hz, β-H), 8.79 (d, 4H, J = 6.0 Hz, py-H$_m$, β-H), 8.13 (d, 2H, J = 8.0 Hz, 15-phenyl-H$_o$), 7.91 (d, 4H, J = 7.7 Hz, 10,20-phenyl-H$_o$), 7.61 (d, 2H, J = 8.0 Hz, 15-phenyl-H$_m$), 7.28 (d, 4H, J = 7.7 Hz, 10,20-phenyl-H$_m$), 2.72 (s, 3H, Me on 15-phenyl), 2.45 (s, 6H, Me on 10,20-phenyl), 1.52 (s, 2H, H_2O), −2.76 (s, 2H, internal N*H*). UV−vis (CH_2Cl_2, nm): 422 (Soret), 518, 556, 592, 650. Anal. Calcd (found) for $C_{186}F_6H_{140}N_{20}O_6S_2$-Pt·$H_2O$: C, 71.09 (70.89); H, 4.55 (4.45); N, 8.91 (8.67). MS {ESI} Calcd (found) *m*/*e*: 1413 (1413) [M-20Tf]$^{2+}$.

{Pt[Zn(pyPP)]$_4$}(OTf)$_2$. [Pt(CH_3CN)$_4$](OTf)$_2$ (20 mg, 0.030 mmol) and Zn(pyPP) (85 mg, 0.12 mmol) were heated at reflux in toluene (40 mL) for 2 days under argon. The solvent was removed under reduced pressure, and the residue was dissolved in a minimum amount (2−5 mL) of C_6H_6. Diethyl ether and hexane were added (10−15 mL), and the mixture was cooled to −20 °C for 8 h. Filtering and washing the solid with diethyl ether produced a purple powder (85 mg, 88%). ^{1}H NMR (CD_2Cl_2, 300 MHz, ppm): 10.48 (d, 2H, J = 6.3 Hz, py-H$_o$), 9.05 (d, 2H, J = 4.5 Hz, β-H), 9.00 (d, 2H, J = 4.5 Hz, β-H), 8.95 (d, 2H, J = 6.6 Hz, β-H), 8.93 (d, 2H, J = 6.6 Hz, β-H), 8.80 (d, 2H, J = 6.3 Hz, py-H$_m$), 8.26 (d, 2H, J = 6.3 Hz, 15-phenyl-H$_o$), 8.10 (m, 4H, 10,20-phenyl-H$_o$), 7.80 (m, 3H, 15-phenyl-H$_{m,p}$), 7.56 (m, 6H, 10,20-phenyl-H$_{m,p}$). UV−vis (CH_2Cl_2, nm): 420 (Soret), 552, 600.

X-ray Crystal Structure Determination of [Pd(DPPP)(H$_2$-pyTP)$_2$](OTf)$_2$. Crystals of [Pd(DPPP)(H$_2$pyTP)$_2$](OTf)$_2$ suitable for single-crystal X-ray diffraction were grown by layering a $CHCl_3$ solution of [Pd(DPPP)(H$_2$pyTP)$_2$](OTf)$_2$ with ethanol. A red-maroon crystal (0.20 × 0.10 × 0.075 mm^3) was mounted on a glass fiber on a Siemens P4 rotating anode diffractometer for data collection at 213 ± 2 K. The cell constants for the data collection were determined from reflections found from a 360° rotation photograph. Twenty-five reflections in the range of 20−25° θ were used to determine precise cell constants.

Lorentz and polarization corrections were applied. A nonlinear correction based on the decay in the standard reflections was also applied to the data. A series of azimuthal reflections was collected. A semiempirical absorption correction based on ψ-scan data was applied to the data.

The space group $P2_1/n$ was chosen on the basis of systematic absences and intensity statistics. This assumption proved to be correct as determined by a successful direct-methods solution[18] and subsequent refinement. All non-hydrogen atoms associated with the porphyrin rings along with Pd and P were found from the initial E-map. All subsequent non-hydrogen atoms were placed from successive difference Fourier maps. All non-hydrogen atoms of the major molecule were refined with anisotropic displacement parameters. The SO_3 moiety of the triflate counterions was refined anisotropically while the CF_3 fragments were refined isotropically with constrained C−F distances. The ethanol and water solvate molecules were also refined isotropically. This refinement scheme was used due to the large amount of thermal motion that the counter/ion and solvent molecules exhibited. All hydrogens were treated as riding atoms with individual isotropic displacement parameters. Final refinements were done with SHELXL-93.[19,20]

Data collection and structure solution were conducted at the Iowa State Molecular Structure Laboratory. Refinement calculations were performed on a Digital Equipment Micro VAX 3100 computer using the SHELXTL-PLUS[18] and SHELXL-93[19] programs.

Results and Discussion

Square Planar d^8 Metals as Linking Reagents. Our approach to constructing new supramolecular arrays focused on new rigid spacer units for covalently linking donor/acceptor assemblies. In addition, porphyrin subunits were chosen since metalation and/or functionalization of the periphery allows the possibility of tuning properties of the assembly. Moreover, porphyrins are closely related to the tetrapyrrolic-type pigments that occur in natural reaction centers. A key aspect of our strategy utilized metal coordination environments as a structural feature that serves to organize the entire assembly. This should allow control of the topology of the multicomponent system. This type of approach has also been employed to link two electroactive molecules to a single metal center.[21] As an initial tactic, we utilized the well-defined and versatile chemistry of square planar Pt(II) and Pd(II) coordination. The precursor metal d^8 complexes which are used to construct the supramolecular framework, *cis*-Pt(DMSO)$_2$Cl$_2$ and *trans*-Pd(DMSO)$_2$Cl$_2$, are well-known starting materials for preparing a wide variety of square planar coordination complexes.[22] The fixed stereochemical relationship of the coordination sites will be used to control the geometric configuration of supramolecular assemblies.

On the basis of the large range of amine complexes of Pt(II) and Pd(II),[23] our initial work began wth an aniline-substituted

Scheme 1

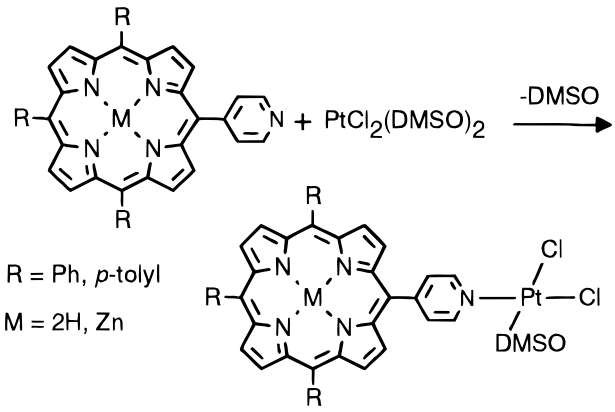

porphyrin, 5-(*p*-aminophenyl)-10,15,20-triphenylporphyrin, H$_2$-TPP-NH$_2$.[24] However, complexes of the aniline derivatives were too difficult to isolate or purify to warrant further study. For example, treatment of *trans*-Pd(DMSO)$_2$Cl$_2$ with excess H$_2$-TPP-NH$_2$ did not produce isolable aniline-ligated porphyrin−Pd complexes. However, when *cis*-Pt(DMSO)$_2$Cl$_2$ was treated with excess H$_2$TTP-NH$_2$ only a monosubstituted complex, *cis*-Pt(NH$_2$-TPPH$_2$)(DMSO)Cl$_2$, was observed as a major species by ^{1}H NMR. This product decomposed on attempted purification by chromatography. Consequently, the aniline-substituted porphyrin was abandoned for the more strongly coordinating pyridyl porphyrins, 5-(*p*-pyridyl)-10,15,20-triphenylporphyrin, (pyPP)H$_2$, and 5-(*p*-pyridyl)-10,15,20-tri(*p*-tolyl)porphyrin, (pyTP)-H$_2$. These functionalized porphyrins are readily prepared in reasonable quantities by literature procedures.[13] Moreover, the close relationship of (pyPP)H$_2$ to tetraphenylporphyrin, (TPP)-H$_2$, is useful from the standpoint that both macrocycles should have similar photophysical and electrochemical properties. Thus the prior work with tetraphenylporphyrin-based reaction center models will provide an important reference point for comparison. In addition, insertion of Zn(II) into the porphyrin core is easily accomplished by published procedures to produce (pyPP)Zn.[14]

Pyridylporphyrin metal complexes with a d^8 metal ion coordinated to the pyridyl nitrogen can be readily synthesized by treating the appropriate porphyrin with M(DMSO)$_2$Cl$_2$ (M = Pt, Pd) in refluxing CHCl$_3$. For example, starting with a 1:1 mixture of *cis*-Pt(DMSO)$_2$Cl$_2$ and (pyPP)H$_2$, we have prepared and cleanly isolated the monoporphyrin adduct *cis*-Pt[(pyPP)-H$_2$](DMSO)Cl$_2$ (Scheme 1) in greater than 90% yield after purification by column chromatography on silica. The Zn-chelated porphyrin (pyPP)Zn can also bind to Pt(II) through the pyridyl nitrogen to form *cis*-Pt[(pyPP)Zn](DMSO)Cl$_2$ in a similar yield. In contrast to the aniline porphyrin analogues, these pyridyl porphyrin complexes are very robust. The complexes remain intact in solution for weeks and in the solid state for more than one year.

^{1}H NMR spectroscopy provides a convenient means of characterizing these products. Thus, the integrated NMR spectrum of *cis*-Pt(DMSO)[(pyPP)H$_2$]Cl$_2$ clearly shows only one coordinated dimethyl sulfoxide ligand (3.6 ppm, s, 6H) and one pyridyl porphyrin bound to Pt. The two-proton singlet at −2.83 ppm is diagnostic for the internal pyrrole protons of the porphyrin and clearly indicates that the Pt(II) ion has not inserted

(18) SHELXTL-PLUS, Siemens Analytical X-ray, Inc., Madison, WI.
(19) SHELXL-93, G. M. Sheldrick, *J. Appl. Cryst*., manuscript in preparation.
(20) All X-ray scattering factors and anomalous dispersion terms were obtained from the *International* Tables for Crytallography; Vol. C, pp 4.2.6.8 and 6.1.1.4.
(21) (a) Miller, T. M.; Ahmed, K. J.; Wrighton, M. S. *Inorg. Chem.* **1989**, *28*, 2347. (b) Carugo, O.; De Santis, G.; Fabbrizzi, L.; Licchelli, M.; Monichino, A.; Pallavicini, P. *Inorg. Chem.* **1992**, *31*, 765. (c) De Blas, A. M.; De Santis, G.; Fabbrizzi, L.; Licchelli, M.; Pallavicini, P.; Poggi, A. In *Supramolecular Chemistry*; Balzani, V., De Cola, L., Eds.; Kluwer Academic: Dordrecht, The Netherlands, 1992; p 87.
(22) Annibale, G.; Bonivento, M.; Canovese, L.; Cattalini, L.; Michelon, G.; Tobe, M. L. *Inorg. Chem.* **1985**, *24*, 797.
(23) (a) Roundhill, M. D. In *Comprehensive Coordination Chemistry*; Wilkinson, G., Ed.; Pergamon Press: Oxford, UK, 1987; Vol. 5, Chapter 52, pp 351−531. (b) Russell, M. J. H.; Barnard, C. F. J. In *Comprehensive Coordination Chemistry*; Wilkinson, G., Ed.; Pergamon Press: Oxford, UK, 1987; Vol. 5, Chapter 51, pp 1099−1130.
(24) Kruper, W. J., Jr.; Chamberlin, T. A.; Kochanny, M. *J. Org. Chem.* **1989**, *54*, 2753.

Scheme 2

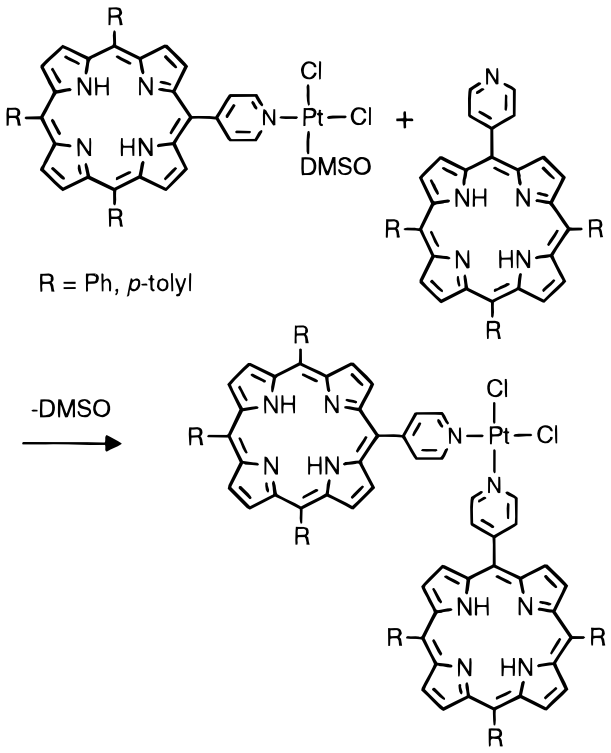

into the porphyrin hole. Moreover, the resonance of the *o*-protons of the pyridyl group has shifted downfield to 9.17 ppm (d, 2H), confirming that the porphyrin subunit is linked to Pt through the desired pyridine functionality. The *o*-protons of the pyridyl group of free (pyPP)H_2 appear at 9.00 ppm. As a means of simplifying the NMR spectrum of the porphyrin fragment of these assemblies, we have also prepared the *p*-tolyl porphyrin analogues from (pyTP)H_2 and (pyTP)Zn.

The absorption spectra of the monomeric porphyrin complexes are also informative. The Soret band for (pyTP)H_2 appears at 418 nm, and the Q-bands occur at 514, 548, 588, and 646 nm. In the complexed form, *cis*-Pt[(pyTP)H_2](DMSO)Cl_2, the absorption bands are virtually unchanged and appear at 422 (Soret), 518, 554, 592, and 648 nm. Thus, the platinum linkage does not significantly perturb the electronic properties of the porphyrin ring.

Two-Component Assemblies. With Pt(II) as the inorganic linkage, the desired monoporphyrin complex can be easily isolated in pure form. Contamination due to formation of the bis-substituted complex is readily avoided. Due to the substitution properties of Pt(II), it is possible to attach additional components in a straightforward manner. Replacement of the second DMSO ligand requires slightly higher reaction temperatures. Thus, treatment of *cis*-Pt[(pyPP)H_2](DMSO)Cl_2 with a second equivalent of (pyPP)H_2 in refluxing toluene results in the clean formation of *cis*-Pt[(pyPP)H_2]$_2Cl_2$ (Scheme 2). The ability of the bisporphyrin complex to withstand higher temperatures reflects the robust nature of these assemblies in solution. An alternate synthesis of the bisporphyrin Pt complex involves heating *cis*-Pt(DMSO)$_2Cl_2$ and 2 equiv of (pyPP)H_2 in refluxing toluene for 36 h. Proton NMR studies show that no bound DMSO is present in the product and that Pt has not inserted into the porphyrin core. The analogues in which the porphyrins are metalated with Zn can be made by two routes. For example, the mono-DMSO adduct, *cis*-Pt[(pyPP)Zn](DMSO)Cl_2, can be treated with a second equivalent of (pyPP)Zn. Alternatively, treatment of *cis*-Pt[(pyPP)H_2]$_2Cl_2$ with excess Zn(OAc)$_2$ produced the Zn metalated product, *cis*-Pt[(pyPP)Zn]$_2Cl_2$.

When Pd(II) is used as the linking reagent, complete substitution of the labile ligands occurs. For example, treating *trans*-Pd(DMSO)$_2Cl_2$ with 1 equiv of (pyPP)H_2 in refluxing $CHCl_3$ resulted in a product mixture which contained a 1:1 ratio of the disubstituted porphyrin−Pd assembly, *trans*-Pd[(pyPP)-H_2]$_2Cl_2$, and bis-DMSO starting material. Treatment of *trans*-Pd(DMSO)$_2Cl_2$ with 2 equiv of pyridyl porphyrin allows preparation and isolation of the pure bisporphyrin assembly, *trans*-Pd[(pyPP)H_2]$_2Cl_2$, in 95% yield. Unfortunately, the lability of the DMSO ligands on Pd will not allow stepwise displacement reactions to form mixed component systems. The Zn porphyrin analogue, Pd[(pyPP)Zn]$_2Cl_2$, can be prepared in a similar manner but has very low solubility in most organic solvents. However, it is soluble in the strongly coordinating solvent pyridine. The tolyl porphyrin derivative, Pd[(pyTP)-H_2]$_2Cl_2$, has similar properties. The bisporphyrin Pd complexes are also robust and have remained unchanged in solution for weeks and in the solid state for more than one year.

The ^{1}H NMR spectra of (pyTP)H_2 and Pd[(pyTP)H_2]$_2Cl_2$ exhibit subtle differences. The monopyridylporphyrin has C_{2v} symmetry and possesses four types of β-pyrrole protons and two kinds of tolyl groups. The inequivalence of the β-pyrrole protons in all of the monopyridylporphyrins is manifested in a complex signal observed in the β-H region. In (pyTP)H_2, the pyrrole proton signals appear as a doublet (8.89 ppm, 2H, J = 4.8 Hz), singlet (8.85 ppm, 4H), and doublet (8.75 ppm, 2H, J = 4.8 Hz). Unexpectedly, all of the tolyl substituents of the unbound ligand have coincidental resonances for the three types of protons: H_o (8.07, 6H, d, J = 7.5 Hz), H_m (7.54, 6H, d, J = 7.5 Hz), and *p*-CH_3 (2.69, 9H, s). However, when the pyridyl group is bound to Pd(II), resonances for the unique tolyl group at the 15-position become distinct from those of the two tolyl substituents at the 10,20-positions. This is illustrated by the two *p*-CH_3 singlets at 2.72 (6H) and 2.70 ppm (3H) for the two types of tolyl groups. In addition, the H_o protons resonate as a pair of overlapping doublets at 8.10 and 8.08 ppm. Overlapping doublets for the H_m protons are also observed at 7.58 and 7.55 ppm. Particularly diagnostic for the formation of Pd[(pyTP)-H_2]$_2Cl_2$ is the large downfield shift (0.38 ppm) of the protons *ortho* to nitrogen on the pyridyl ring to 9.38 ppm.

It is well-known that Pd(L)$_2Cl_2$ complexes prefer *trans* geometries and that Pt(L)$_2Cl_2$ complexes prefer *cis* configurations.[15,22] The *trans* geometry for Pd[(pyPOR)H_2]$_2Cl_2$ was verified by far-IR studies. For example, Pd[(pyPP)H_2]$_2Cl_2$ has only one Pd−Cl stretch found at 367 cm^{-1}. The *cis* configuration for Pt[(pyPP)H_2]$_2Cl_2$ was established from two observed Pt−Cl vibrations found at 354 and 324 cm^{-1}.

The stepwise replacement of ligands at Pt(II) allows the possibility of fabricating multicomponent assemblies in a systematic manner. To demonstrate this propsect we sought to prepare mixed component assemblies. It is clear that the appended components must be attached to suitable ligands. The quinone derived from isoquinoline, benz[*g*]isoquinoline-5,10-dione, seemed to be an ideal subunit for attachment to a Pt−porphyrin assembly. Unfortunately, we were unsuccessful in binding this quinone to *cis*-Pt[(pyTP)H_2](DMSO)Cl_2 or *cis*-Pt-[(pyTP)Zn](DMSO)Cl_2. However, 4-pyridyl-4′-methylpyridinium iodide (monoquat, MQ^+I^-) was a well-behaved ligand which allowed the preparation of robust two-component assemblies. Thus, treatment of *cis*-Pt(pyPOR)(DMSO)Cl_2 with 1 equiv of MQ^+I^- in refluxing THF/EtOH solutions cleanly produced the *cis*-porphyrin−Pt−viologen assemblies in 50−70% yields (Scheme 3). These two-component arrays were prepared with (pyPP)H_2, (pyTP)H_2, (pyPP)Zn, and (pyTP)Zn. ^{1}H NMR spectroscopy provides a useful tool for monitoring

Scheme 3

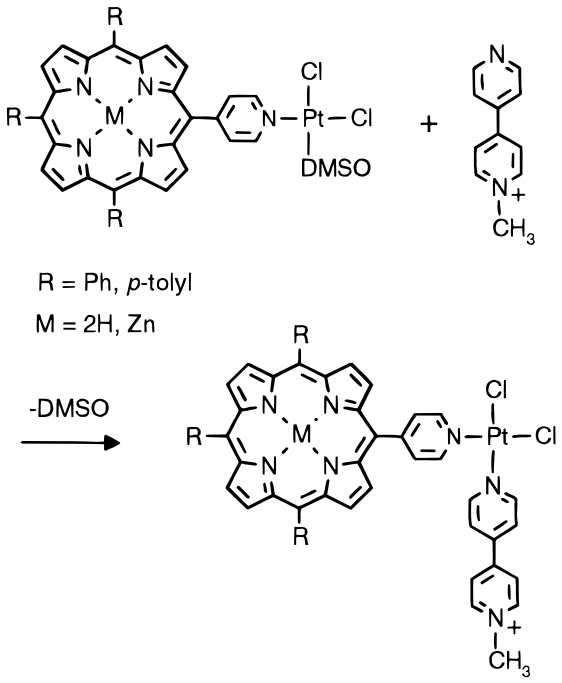

Scheme 4

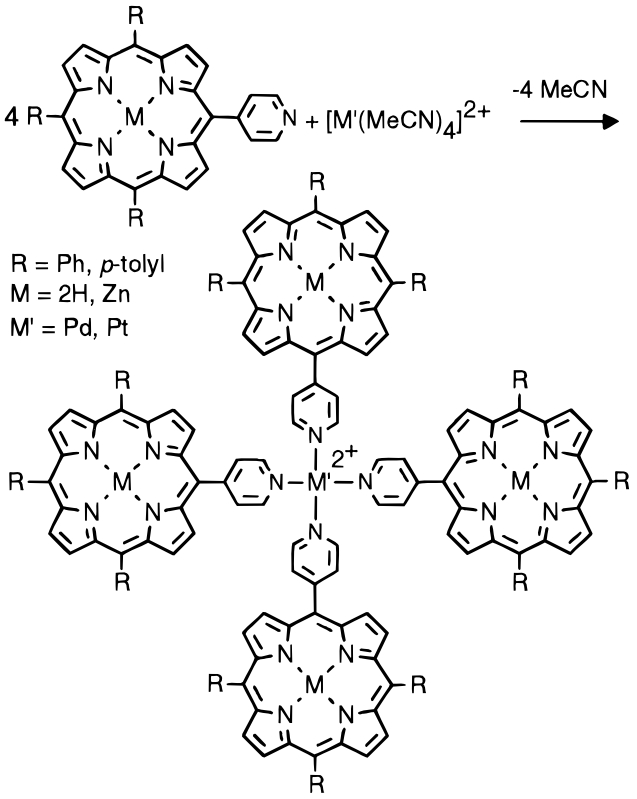

the reactions. Again, formation of the product is signified by the loss of the resonance at 3.6 ppm for coordinated DMSO. Furthermore, a new signal for the bound MQ^+ ligand appears at 4.5−4.8 ppm (3H, s, MQ-Me). The methyl signal for unbound MQ^+ resonates at 4.25 ppm. However, the NMR spectrum for these mixed assemblies is more complex due to the addition of four new resonances in the aromatic region from the bound MQ^+ ligand. Unambiguous assignments were made with the aid of 2D-COSY ^{1}H NMR. Thus, peaks at 8.97 (d, 2H, J = 5.4 Hz, MQ-H_o), 8.89 (d, 2H, J = 5.6 Hz, MQ-$H_{o'}$), 8.19 (d, 2H, J = 5.4 Hz, MQ-H_m), 7.59 (d, 2H, J = 5.6 Hz, MQ-$H_{m'}$) were assigned to the bound MQ^+ ligand of *cis*-Pt[(pyTP)H_2](MQ^+I^-)Cl_2.

Preparation of mixed bisporphyrin assemblies proved to be more difficult. For example, treatment of Pt(DMSO)[(pyPP)-H_2]Cl_2 with 1 equiv of (pyTP)Zn produced the three bisporphyrin complexes Pt[(pyTP)Zn]$_2Cl_2$, Pt[(pyPP)H_2]$_2Cl_2$, and Pt[(pyTP)Zn][(pyPP)H_2]Cl_2 as observed by ^{1}H NMR. All three species have very similar mobilities on chromatography supports, and we have not been able to separate them.

Four-Component Assemblies. As a means of illustrating the versatility of using transition metal reagents as rigid spacers, we sought to link the maximum number of components to a single center. For Pd(II) and Pt(II) ions, the square planar coordination properties allow the organization of four subunits in a supramolecular assembly. Tetrakisporphyrin complexes can be prepared readily in a one-pot synthesis. Thus, the reaction of excess (pyTP)H_2 or (pyPP)Zn with [M(CH_3CN)$_4$]-X_2 (M = Pt, Pd; X = BF_4, OTf) leads to the formation of tetrasubstituted complexes, M[(pyPOR)H_2]$_4^{2+}$, as shown in Scheme 4. The ^{1}H NMR spectra of these complexes confirm the composition and general structure of the assembly. Each complex exhibits only one set of porphyrin resonances. For example, in [Pt{(pyTP)H_2}$_4$](OTf)$_2$, all of the protons *ortho* to the pyridyl nitrogens appear as a single resonance (10.52 ppm, d, J = 6.0 Hz). In addition, the tolyl methyl protons give rise to only two singlets, 2.72 (s, 3H) and 2.45 (s, 6H), which can be assigned to the two symmetry-inequivalent types of tolyl groups on a single ligand. This indicates that all four porphyrins around the metal ion are identical on the NMR time scale and that the Pt and Pd ions have square planar environments in solution. The tetrapyridine Pd(II) analogue, [Pd(py)$_4$]$^{2+}$, has a similar coordination geometry.[25]

The exact structures of these novel tetrakisporphyrin supramolecular assemblies are of considerable interest. However, we have not yet been able to grow suitable crystals of these complexes for X-ray diffraction. Nonetheless, it is unlikely that all four porphyrin macrocycles can achieve a coplanar arrangement about the central metal ion because of steric constraints. On the basis of the structure of the Pd(DPPP) bisporphyrin complex (see below), the tetrakisporphyrin assembly probably adopts a propeller-type configuration with twist angles of approximately 30°.

The absorption and emission spectra of the porphyrin complexes show that there are only very limited changes between the free porphyrin and the porphyrin−metal assemblies. In the UV−vis spectra, the bisporphyrin assembly, *cis*-Pt-[(pyPP)H_2]$_2Cl_2$, showed a slight red-shift in absorption bands, relative to the unbound pyridyl porphyrin, to 420 (Soret), 516, 552, 590, and 646 nm. In the emission spectra, (pyPP)H_2 has peaks at 652 and 714, while the Pt and Pd complexes Pt(DMSO)[(pyPP)H_2]Cl_2, Pt[(pyPP)H_2]$_2Cl_2$, Pt[(pyPP)H_2]-(MQ^+I^-)Cl_2, and Pd[(pyPP)H_2]$_2Cl_2$ essentially have the same emission peak positions. This observation is also true for the case of (pyTP)H_2 and their Zn porphyrins Pd(II) and Pt(II) complexes. Consequently, the Pd and Pt centers do not strongly couple the subunits electronically and thus serve primarily as structural components.

Structural Studies. Due to the relationship of these porphyrin assemblies to photosynthetic electron transfer models, structures are of considerable interest. However, the dichloro Pt− and Pd−porphyrin assemblies have relatively low solubilities in organic solvents and growing X-ray-quality single crystals was difficult. In general, these complexes precipitated as

(25) Siedle, A. R.; Pignolet, L. H. *Inorg. Chem.* **1982**, *21*, 135.

Scheme 5

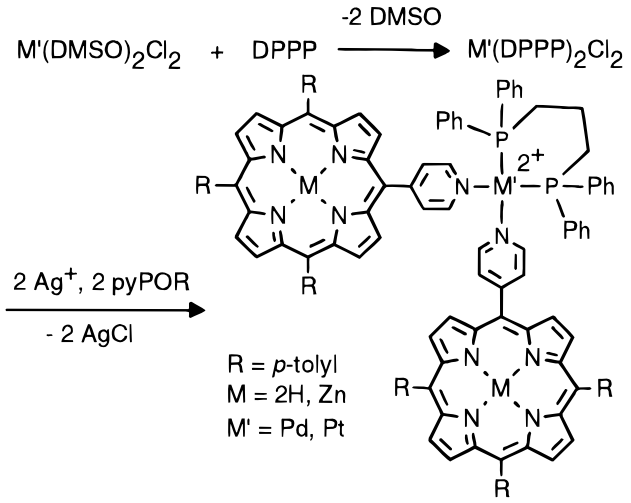

powders or as microcrystals. For achieving higher solubility, platinum and palladium compounds containing the chelate ligand 1,3-bis(diphenylphosphino)propane (DPPP), were employed as starting materials. Treating Pt(DPPP)Cl_2 and Pd(DPPP)Cl_2 with 2 equiv of silver triflate generates M(DPPP)$(OTf)_2$.[26] Substitution of the triflate ligands with monopyridylporphyrins produced only bisporphyrin complexes. Treatment of M(DPPP)$(OTf)_2$ with 1 equiv of monopyridylporphyrin results in a mixture of bisporphyrin complexes and unreacted starting material. Scheme 5 illustrates the synthesis of DPPP bisporphyrin assemblies. The diphosphine complexes, [M(DPPP){(pyTP)H_2}$_2$](OTf)$_2$, are soluble in common organic solvents such as C_6H_6, toluene, acetone, CH_2Cl_2, and $CHCl_3$ and have much higher solubility compared with the chloride analogues, M[(pyPOR)H_2]$_2Cl_2$.

The ^{1}H NMR spectra for the DPPP bisporphyrin complexes retain features similar to those observed for the nonchelate analogues. For example, in {Pd(DPPP)[(pyTP)H_2]$_2$}(OTf)$_2$, the *o*-pyridyl protons appear far downfield at 9.61 ppm (d, 4H). The use of 2D-COSY was used to identify the remaining aromatic resonances to avoid confusion due to the large extent of overlapping signals. For example, the *m*-pyridyl protons (4H), the *o*-tolyl protons (12H), and the *o*-phenyl-DPPP protons (8H) resonate as a large 24-H multiplet at 8.08 ppm. In addition, one set of β-pyrrole protons appears much further upfield (8.22 ppm) than typically observed.

^{31}P NMR spectroscopy of the DPPP complexes also provides a useful means of characterization. For the Pd complexes, a single ^{31}P resonance was observed at 5.28−6.91 ppm. Similarly, the Pt analogues exhibit a single ^{31}P resonance at −15.0 to −16.47 ppm. These values are typical of those observed for related DPPP Pd and Pt complexes.[27]

Crystals of [Pd(DPPP){(pyTP)H_2}$_2$](OTf)$_2$ suitable for X-ray diffraction were prepared by layering ethanol on top of a $CHCl_3$ solution. The molecular structure of [Pd(DPPP){(pyTP)H_2}$_2$]-(OTf)$_2$ was determined by single-crystal X-ray diffraction. The molecular structure and atom numbering scheme are shown in Figure 1. Crystallographic data for the structure determination are listed in Table 1. Atomic positional parameters are given in Table 2. Bond distances and angles are listed in Table 3.

[Pd(DPPP){(pyTP)H_2}$_2$](OTf)$_2$ crystallizes in the space group $P2_1/n$ with four molecules per unit cell. As expected, the Pd(II) ion has a pseudo-square-planar geometry. Two *cis* sites

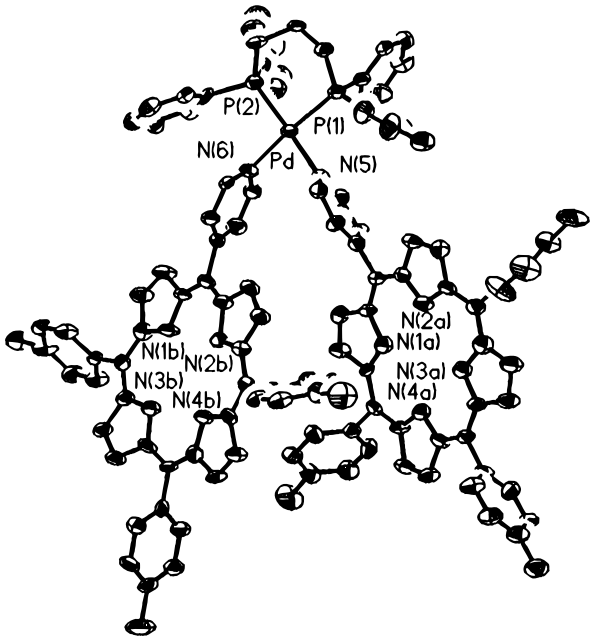

Figure 1. Molecular structure for [Pd(DPPP){(pyTP)H_2}$_2$](OTf)$_2$. Thermal ellipsoids are drawn at the 50% probability level.

Table 1. Structure Determination Summary for [Pd(DPPP)[(pyTP)H_2]$_2$](OTf)$_2$[a]

empirical formula	$C_{123}H_{104}F_6N_{10}O_8P_2PdS_2$
color, habit	red-maroon, rectangular prism
crystal size (mm)	0.2 × 0.1 × 0.075
crystal system	monoclinic
space group	$P2_1/n$
unit cell dimensions	
a (Å)	13.211(5)
b (Å)	36.741(19)
c (Å)	22.971(10)
β (deg)	91.54(3)
V (Å)^3	11145.8(86)
Z	4
fw	2196.62
density (calc) (Mg/m^3)	1.309
absorption coefficient (mm^{-1})	2.554
F(000)	4552
diffractometer used	Siemens P4 Rotating Anode
radiation (λ, Å)	Cu Kα (1.54178)
temperature (K)	213(2)
monochromator	graphite
θ range	3.08−56.75°
scan type	$2\theta-\theta$
reflections collected	17837
independent reflections	14901 (R_{int} = 0.0826)
observed reflections	5252 ($I \geq 2\sigma(I)$)
parameters refined	1313
final R indices [$I \geq 2\sigma(I)$]	$R1$ = 0.0821, $wR2$ = 0.1844
R indices (all data)	$R1$ = 0.1964, $wR2$ = 0.2183
GooF, observed and all data	1.269, 0.824
largest and mean Δ/σ	1.007, 0.018
largest difference peak (e/Å^{-3})	0.877
largest difference hole (e/Å^{-3})	−0.633

[a] $R1 = \sum||F_o| - |F_c|| / \sum|F_o|$. $wR2 = [\sum[w(F_o^2 - F_c^2)^2] / \sum[w(F_o^2)^2]]^{0.5}$, where $w = 1/[\sigma^2(F_o^2) + (a*P)^2 + b*P + d + e*/\sin\theta]$. GooF $= [\sum[w(F_o^2 - F_c^2)^2]/(n-p)]^{0.5}$.

are occupied by the DPPP ligand and the remaining two sites are taken up by the pyridyl porphyrins. The bond angles around the palladium(II) ion are close to the expected value of 90°, ranging from 83.4(3)° to 94.2(2)°. The P−Pd−P chelate angle is 90.22(11)°, and the N−Pd−N angle is 83.4(3)°. The Pd−N distances (2.095(9) and 2.112(9) Å) are in the range of those observed for other bispyridine palladium(II) complexes.[28] The Pd−P distances (2.247(3) and 2.258(3) Å) are also in the normal

(26) Stang, P. J.; Cao, D. H.; Poulter, G. T.; Arif, A. M. *Organometallics* **1995**, *14*, 1110.
(27) Stang, P. J.; Cao, D. H.; Saito, S.; Arif, A. M. *J. Am. Chem. Soc.* **1995**, *117*, 6273.

Table 2. Atomic Coordinates ($\times 10^4$) and Equivalent Isotropic Displacement Parameters ($Å^2 \times 10^3$) for $[Pd(DPPP)[(pyTP)H_2]_2(OTf)_2$

atom	*x*	*y*	*z*	*U*(eq)[a]	atom	*x*	*y*	*z*	*U*(eq)[a]
Pd	6960(1)	117(1)	7636(1)	36(1)	C(37A)	2948(10)	−4123(3)	9071(6)	57(4)
P(1)	5892(2)	403(1)	8236(1)	39(1)	C(38A)	3333(9)	−3782(3)	8943(6)	56(4)
P(2)	7461(2)	657(1)	7284(1)	40(1)	C(39A)	2834(10)	−4674(3)	9704(6)	73(4)
N(5)	6519(7)	−400(2)	7938(4)	37(2)	C(40A)	8473(9)	−2801(3)	8415(5)	37(3)
N(6)	7931(7)	−187(2)	7118(4)	37(2)	C(41A)	9129(9)	−2944(3)	8831(5)	47(3)
N(1A)	6348(7)	−2114(2)	8581(4)	40(3)	C(42A)	10061(9)	−3081(3)	8686(6)	53(4)
N(2A)	4310(7)	−1869(2)	8806(4)	40(3)	C(43A)	10351(10)	−3071(3)	8108(6)	55(4)
N(3A)	3762(7)	−2590(2)	9155(4)	45(3)	C(44A)	9716(9)	−2924(3)	7685(6)	52(4)
N(4A)	5784(7)	−2844(2)	8911(4)	39(3)	C(45A)	8777(9)	−2794(3)	7843(5)	47(3)
N(1B)	10468(7)	−1553(2)	6066(4)	45(3)	C(46A)	11383(9)	−3225(4)	7979(6)	85(5)
N(2B)	8451(7)	−1824(2)	6364(4)	40(3)	C(1B)	11451(9)	−1483(3)	5894(5)	42(3)
N(3B)	11006(7)	−2285(2)	5726(4)	40(3)	C(2B)	11652(9)	−1104(3)	6005(6)	51(4)
N(4B)	9001(7)	−2543(2)	6074(4)	39(3)	C(3B)	10804(9)	−952(3)	6219(6)	53(4)
C(101)	5208(8)	786(3)	7935(5)	44(3)	C(4B)	10058(9)	−1234(3)	6275(5)	37(3)
C(102)	5904(9)	1087(3)	7715(5)	47(4)	C(5B)	9064(9)	−1188(3)	6448(5)	38(3)
C(103)	6459(9)	984(3)	7154(5)	50(4)	C(6B)	8323(8)	−1456(3)	6490(5)	36(3)
C(104)	6563(9)	563(3)	8874(5)	35(3)	C(7B)	7312(8)	−1401(3)	6701(5)	49(4)
C(105)	6169(9)	832(3)	9228(5)	39(3)	C(8B)	6843(9)	−1726(3)	6688(5)	45(3)
C(106)	6704(9)	936(3)	9718(5)	45(3)	C(9B)	7557(10)	−1985(3)	6479(5)	45(3)
C(107)	7613(10)	789(4)	9879(6)	62(4)	C(10B)	7354(8)	−2358(3)	6434(5)	34(3)
C(108)	7995(10)	510(3)	9532(6)	59(4)	C(11B)	8047(9)	−2619(3)	6250(5)	37(3)
C(109)	7479(9)	405(3)	9039(5)	46(3)	C(12B)	7915(9)	−3011(3)	6251(5)	46(3)
C(110)	4896(8)	106(3)	8493(5)	40(3)	C(13B)	8746(8)	−3163(3)	6082(5)	40(3)
C(111)	4992(9)	−57(3)	9025(6)	50(3)	C(14B)	9465(9)	−2875(3)	5955(5)	40(3)
C(112)	4202(10)	−273(3)	9226(6)	52(4)	C(15B)	10421(9)	−2918(3)	5740(5)	41(3)
C(113)	3346(11)	−318(3)	8893(7)	64(4)	C(16B)	11099(9)	−2652(3)	5606(5)	42(3)
C(114)	3284(10)	−160(4)	8368(6)	76(5)	C(17B)	12022(9)	−2690(3)	5292(5)	49(4)
C(115)	4038(10)	56(3)	8155(6)	63(4)	C(18B)	12486(9)	−2366(3)	5267(5)	46(3)
C(116)	8407(9)	887(3)	7697(5)	45(3)	C(19B)	11868(9)	−2106(3)	5551(5)	43(3)
C(117)	8536(11)	1267(3)	7673(6)	65(4)	C(20B)	12083(8)	−7636(3)	5643(5)	38(3)
C(118)	9330(14)	1429(4)	7977(8)	87(5)	C(21B)	8765(9)	−807(3)	6644(5)	39(3)
C(119)	9957(13)	1234(5)	8343(8)	94(6)	C(22B)	9201(10)	−648(3)	7121(5)	50(3)
C(120)	9898(13)	849(5)	8373(7)	91(5)	C(23B)	8746(9)	−335(3)	7347(5)	42(3)
C(121)	9045(11)	694(4)	8053(6)	61(4)	C(24B)	7563(9)	−320(3)	6616(5)	42(3)
C(122)	8012(11)	589(3)	6572(5)	46(3)	C(25B)	7938(9)	−638(3)	6357(5)	43(3)
C(123)	7424(11)	566(3)	6080(6)	53(4)	C(26B)	6327(9)	−2491(3)	6568(5)	39(3)
C(124)	7853(10)	496(3)	5551(6)	54(4)	C(27B)	5945(9)	−2458(3)	7128(6)	52(4)
C(125)	8863(12)	439(3)	5512(7)	61(4)	C(28B)	4950(11)	−2570(3)	7227(7)	60(4)
C(126)	9462(12)	460(4)	6019(7)	73(5)	C(29B)	4328(10)	−2695(3)	6804(7)	56(4)
C(127)	9056(9)	536(3)	6551(6)	52(4)	C(30B)	4674(9)	−2727(3)	6251(6)	51(4)
C(1A)	7260(8)	−2289(3)	8481(5)	31(3)	C(31B)	5667(9)	−2625(3)	6135(6)	46(3)
C(2A)	7950(9)	−2030(3)	8255(5)	47(3)	C(32B)	3264(9)	−2814(4)	6932(7)	94(6)
C(3A)	7479(8)	−1709(3)	8209(5)	43(3)	C(33B)	10777(9)	−3303(3)	5623(5)	37(3)
C(4A)	6465(9)	−1754(3)	8419(5)	39(3)	C(34B)	11349(9)	−3480(3)	6046(6)	45(3)
C(5A)	5708(9)	−1491(3)	8439(5)	38(3)	C(35B)	11716(9)	−3832(3)	5944(6)	52(4)
C(6A)	4701(9)	−1542(3)	8614(5)	41(3)	C(36B)	11548(9)	−4005(3)	5418(6)	49(4)
C(7A)	3955(9)	−1265(3)	8661(5)	49(4)	C(37B)	10943(10)	−3822(3)	4995(6)	56(4)
C(8A)	3107(10)	−1421(3)	8878(5)	47(3)	C(38B)	10592(9)	−3472(3)	5100(6)	50(4)
C(9A)	3334(9)	−1795(3)	8978(5)	37(3)	C(39B)	11961(11)	−4385(3)	5310(7)	92(5)
C(10A)	2689(9)	−2048(3)	9236(5)	43(3)	C(40B)	13108(9)	−1604(3)	5469(5)	39(3)
C(11A)	2889(9)	−2413(3)	9323(6)	49(3)	C(41B)	13986(10)	−1753(3)	5688(6)	53(4)
C(12A)	2230(10)	−2673(3)	9583(6)	71(5)	C(42B)	14894(10)	−1624(3)	5540(6)	57(4)
C(13A)	2678(10)	−3004(3)	9565(6)	62(4)	C(43B)	15015(9)	−1337(3)	5165(6)	49(4)
C(14A)	3629(9)	−2952(3)	9286(5)	47(4)	C(44B)	14138(9)	−1193(3)	4921(5)	50(4)
C(15A)	4342(10)	−3219(3)	9213(5)	47(4)	C(45B)	13191(9)	−1318(3)	5068(5)	49(3)
C(16A)	5339(9)	−3175(3)	9039(5)	41(3)	C(46B)	16040(8)	−1178(3)	5018(6)	63(4)
C(17A)	6076(9)	−3462(3)	8973(5)	43(3)	S(1)	4570(3)	168(1)	6387(2)	60(1)
C(18A)	6935(10)	−3299(3)	8813(5)	46(3)	O(1)	5395(6)	117(2)	6795(3)	64(2)
C(19A)	6762(9)	−2918(3)	8776(5)	38(3)	O(2)	4728(7)	437(3)	5970(4)	101(4)
C(20A)	7445(8)	−2661(3)	8572(5)	34(3)	O(3)	3593(7)	163(3)	6623(4)	97(3)
C(21A)	5986(10)	−1110(3)	8254(5)	45(3)	C(1S)	4757(15)	−347(6)	5955(9)	134(8)
C(22A)	6784(8)	−927(3)	8538(5)	38(3)	F(1)	3924(9)	−272(3)	5610(5)	147(4)
C(23A)	7027(9)	−572(3)	8358(5)	43(3)	F(2)	5504(11)	−248(4)	5704(6)	193(6)
C(24A)	5768(10)	−575(3)	7675(5)	50(4)	F(3)	4499(11)	−533(4)	6362(7)	207(6)
C(25A)	5478(9)	−935(3)	7807(5)	38(3)	S(2)	10246(4)	−325(2)	8749(3)	143(2)
C(26A)	1695(9)	−1913(3)	9436(6)	43(3)	O(4)	10861(10)	−183(4)	9256(5)	167(6)
C(27A)	1633(9)	−1688(3)	9909(6)	56(4)	O(5)	10735(9)	−350(5)	8180(5)	185(8)
C(28A)	683(10)	−1558(3)	10095(6)	56(4)	O(6)	9247(7)	−157(3)	8750(6)	137(5)
C(29A)	−172(10)	−1646(4)	9848(7)	61(4)	C(2S)	9946(19)	−765(10)	8893(12)	238(14)
C(30A)	−134(10)	−1887(4)	9411(7)	85(5)	F(4)	10846(13)	−950(4)	8890(6)	217(6)
C(31A)	781(12)	−2015(4)	9190(7)	92(6)	F(5)	9588(17)	−712(6)	9463(11)	351(11)
C(32A)	−1206(9)	−1491(3)	10037(7)	88(5)	F(6)	9362(9)	−907(3)	8477(5)	162(5)
C(33A)	3999(9)	−3608(3)	9333(6)	45(3)	C(3S)	1819(16)	−1715(6)	7449(10)	192(10)
C(34A)	4289(10)	−3784(3)	9831(5)	53(4)	C(4S)	962(12)	−2045(4)	7474(7)	97(5)
C(35A)	3885(10)	−4126(3)	9948(6)	53(4)	O(23)	2932(10)	−1798(3)	7304(5)	139(5)
C(36A)	3233(9)	−4298(3)	9570(7)	53(4)	O(50)	1385(22)	−5(8)	7000(13)	420(16)

[a] Equivalent isotropic *U* defined as one-third the trace of the orthogonalized U_{ij} tensor.

Table 3. Selected Bond Lengths (Å) and Angles (deg) for $[Pd(DPPP)[(pyTP)H_2]_2(OTf)_2$

Bond Lengths

Pd−N(6)	2.095(9)	N(4B)−C(14B)	1.395(13)
Pd−N(5)	2.112(9)	C(101)−C(102)	1.533(13)
Pd−P(2)	2.247(3)	C(102)−C(103)	1.547(14)
Pd−P(1)	2.258(3)	C(104)−C(109)	1.387(14)
P(1)−C(104)	1.792(11)	C(104)−C(105)	1.390(13)
P(1)−C(101)	1.799(10)	C(105)−C(106)	1.367(14)
P(1)−C(110)	1.820(11)	C(106)−C(107)	1.36(2)
P(2)−C(116)	1.765(13)	C(107)−C(108)	1.40(2)
P(2)−C(103)	1.806(11)	C(108)−C(109)	1.36(2)
P(2)−C(122)	1.826(12)	C(1A)−C(20A)	1.405(13)
N(5)−C(24A)	1.315(14)	C(1A)−C(2A)	1.424(14)
N(5)−C(23A)	1.322(13)	C(2A)−C(3A)	1.338(14)
N(6)−C(23B)	1.303(13)	C(3A)−C(4A)	1.446(14)
N(6)−C(24B)	1.332(13)	C(4A)−C(5A)	1.395(14)
N(1A)−C(4A)	1.382(12)	C(5A)−C(6A)	1.413(14)
N(1A)−C(1A)	1.389(12)	C(21A)−C(25A)	1.37(2)
N(2B)−C(6B)	1.394(12)	C(21A)−C(22A)	1.40(2)
N(3B)−C(16B)	1.381(12)	C(22A)−C(23A)	1.409(13)
N(3B)−C(19B)	1.385(13)	C(24A)−C(25A)	1.412(14)
N(4B)−C(11B)	1.362(13)		

Bond Angles

N(6)−Pd−N(5)	83.4(3)	P(2)−Pd−P(1)	90.22(11)
N(6)−Pd−P(2)	94.4(2)	C(104)−P(1)−C(101)	106.9(5)
N(5)−Pd−P(2)	177.7(2)	C(104)−P(1)−C(110)	106.1(5)
N(6)−Pd−P(1)	175.3(3)	C(101)−P(1)−C(110)	103.5(5)
N(5)−Pd−P(1)	92.1(2)	C(104)−P(1)−Pd	110.4(4)
C(101)−P(1)−Pd	116.4(4)	C(6A)−C(5A)−C(21A)	116.3(10)
C(110)−P(1)−Pd	112.8(4)	C(25A)−C(21A)−C(22A)	118.3(10)
C(24A)−N(5)−C(23A)	117.7(10)	C(25A)−C(21A)−C(5A)	121.8(12)
C(24A)−N(5)−Pd	120.0(8)	C(22A)−C(21A)−C(5A)	119.9(11)
C(23A)−N(5)−Pd	122.1(8)	C(4B)−C(5B)−C(6B)	127.1(10)
C(23B)−N(6)−C(24B)	118.3(10)	C(4B)−C(5B)−C(21B)	116.7(10)
C(23B)−N(6)−Pd	120.4(8)	C(6B)−C(5B)−C(21B)	116.1(10)
C(24B)−N(6)−Pd	118.1(8)	C(22B)−C(21B)−C(25B)	119.6(11)
C(4A)−N(1A)−C(1A)	107.0(9)	C(22B)−C(21B)−C(5B)	121.7(11)
C(4A)−C(5A)−C(6A)	126.7(10)	C(25B)−C(21B)−C(5B)	118.2(11)
C(4A)−C(5A)−C(21A)	117.0(10)		

range for *cis*-chelating phosphine Pd complexes.[26] The pyridyl planes are nearly orthogonal to the Pd square plane, forming dihedral angles of 86.3° and 88.3°. The triflate ions appear not to bind to the metal ion. The closest approach of a counterion to Pd is O1 with a distance of 2.86 Å.

The metrical parameters for the individual porphyrin ligands show no unusual features. Bond distances and angles are typical for nonmetalated porphyrins. The 24-atom core framework of porphyrin a remains relatively planar with an average out-of-plane displacement of 0.074 Å. The largest displacement is observed for C17a at 0.14 Å. The 24 core atoms of porphyrin b also exhibit a mean displacement from the plane of 0.074 Å. However, porphyrin b is somewhat ruffled in the typical saddle-shaped distortion with pyrrole rings alternately tipping up and down with respect to the mean porphyrin plane. The largest deviation from planarity for porphyrin b is 0.33 Å at C18b.

The mean porphyrin planes are canted with respect to the Pd square plane by 27.6° and 28.5°, presumably to minimize steric interactions of the tolyl groups in the 10,20-positions between porphyrins in the same molecule. Perhaps the most unusual structural aspect in this Pd-linked assembly involves the intramolecular porphyrin separation. From the simple geometric relationship of a 90°-bond angle, the calculated center-to-center distance for two undistorted *cis* ligated pyridyl porphyrins is 13.6 Å. The observed center-to-center distance between the two porphyrin rings is much shorter at 8.69 Å and may be a manifestation of intramolecular $\pi-\pi$ interactions or crystal packing forces in the solid state. Note that in solution, the electronic spectra of the bisporphyrin assemblies show no strong $\pi-\pi$ interactions. In addition, the dihedral angle between the two porphyrin mean planes is only 19.8°. Thus, the porphyrins are strongly distorted toward each other. No significant deformations at pyridyl atoms N5, C21a, N6, and C21b or meso carbons C5a and C5b are associated with this observation. The sum of the bond angles (356.8−360°) at each of these atoms indicates that they all are relatively planar sp^2 centers. However, the two pyridyl planes form a dihedral angle of 55.9° in relation to this distortion.

Concluding Remarks

This work illustrates that transition metal complexes can serve as useful structural linkages to control orientation and distance between subunits in multicomponent assemblies. The design aspects of our approach allow the versatility of using a wide variety of pigments, electron donors, and electron acceptors. A key restriction is that it must be possible to link the desired component to a suitable ligand. For example, pyridines are much better than aniline-type bases for binding to Pt(II) and Pd(II). Pyridylporphyrin ligands generally form inert linkages to Pt(II) and Pd(II). The complexes described here remain intact for weeks in solution and for more than one year in the solid state. We have not yet succeeded in appending a quinone-type acceptor to coordination assemblies. However, an important feature of this strategy is the ease in which complex structures can be fabricated in moderate to high yields. Moreover, the geometry at the metal center allows significant control over spatial orientation and position. For example, in the bisporphyrin assemblies, changing from a *cis*-Pt linkage to a *trans*-Pd spacer produces center-to-center porphyrin distances that change from 8.69 to roughly 19.5 Å, respectively. Mixed component assemblies can be readily prepared as illustrated by the synthesis of four different porphyrin−viologen complexes. In addition, we have demonstrated the facile preparation of four-component supramolecular arrays. In essence, the metal ion can serve as a template for the organization of several subunits. Thus, fabrication of complex systems with well-defined organization can be achieved in a straightforward manner. The strength of this coordinative approach derives from its versatility and promises to complement and supplement the important information gained from organically linked donor/acceptor complexes. The single-crystal X-ray structure of a bisporphyrin complex provides important metrical information for predicting structures of related assemblies. Preparation of other supramolecular assemblies and a study of photophysical properties are the subject of ongoing studies.

Acknowledgment. Financial support of this work was provided by a Carver Trust grant, administered by Iowa State University, funds from the NSF, and a Camille and Henry Dreyfus Teacher−Scholar Award.

Supporting Information Available: A listing of bond lengths, bond angles, anisotropic displacement parameters, and hydrogen coordinates (18 pages). This material is contained in many libraries on microfiche, immediately follows this article in the microfilm version of the journal, can be ordered from the ACS, and can be downloaded from the Internet; see any current masthead page for ordering information and Internet access instructions.

IC951594N

(28) Horike, M.; Kai, Y.; Yasuoka, N.; Kasai, N. *J. Organomet. Chem.* **1975**, *86*, 269.